A Study of the Performance of Wireless Sensor Networks Operating with Smart Antennas

E. D. Skiani, S. A. Mitilineos, and S. C. A. Thomopoulos

National Center for Scientific Research 'Demokritos'
Institute of Informatics & Telecommunications, Integrated Systems Laboratory
Grigoriou 1 and Neapoleos Str., 15310, Athens, Greece
E-mail: vskiani@iit.demokritos.gr; smitil@teipir.gr; scat@iit.thomopoulos.gr

Abstract

Wireless sensor networks (WSNs) have attracted a great deal of research interest during the last few years, with potential applications making them ideal for the development of the envisioned world of ubiquitous and pervasive computing. Energy and computational efficiency constraints are the main key issues when dealing with this type of network. The main research effort has been channeled towards routing and distributed processing, in order to achieve better quality of service (QoS) provisions, lower interference, and a lower power-consumption rate while data dissemination is carried out. The embedment of smart antennas on wireless-sensor nodes is proposed herein as an alternative and novel approach at the physical layer, with the potential for relieving traditional challenges faced by current wireless-sensor-network architectures. Studying the behavior of wireless sensor networks consisting of different types of antennas (omnidirectional or adaptive directional) yielded unexpectedly favorable results that improved the operation of networking systems of this type. In the test cases presented herein, the incorporation of smart antennas resulted in approximate improvements in the quality of service by 20%, the efficiency by 50%, the percentage of active nodes by 20%, and the energy consumption by 50%, depending on the simulation setup.

Keywords: Wireless sensor networks; smart antennas; simulation; quality of service; energy consumption; wireless networks; directional antennas

1. Introduction

Wireless sensor networks (WSNs) are a class of distributed computing and communication systems that are an integral part of the physical space they inhabit [1]. This type of network is characterized by nodes with a low profile, having limited computational power and sparse energy resources, which have the ability to collaborate with each other, and to sense, reason, and react to the world that surrounds them. Recent advances in this field have enabled the development of wireless sensor networks, the functionality of which rely on the collaborative effort of a large number of tiny, low-cost, low-power, multi-functional sensor nodes that are able to communicate un-tethered over short distances [2, 3]. Moreover, engineering or predetermining the positions of the nodes is not necessary. This allows random deployment in hostile environments or disaster-relief operations, a unique feature that accounts for rendering these network types an integral part of modern life. Smart environments represent the next evolutionary development step in the automation of building, utility, industrial, home, shipboard, and transportation systems [4]. This bridge to the physical world has enabled a growing bouquet of added-value services, ranging from health to military and security, such as target tracking, environmental control, habitat monitoring, source detection and localization, vehicular and traffic monitoring, health monitoring, building and industrial monitoring, etc. [5, 6].

On the other hand, wireless sensor networks display certain undesirable or hard-to-deal-with features. These include power limitations, frequently changed topology, broadcast communication, susceptibility to failure, and low memory, while their architecture calls for protocols and algorithms with self-organizing capabilities [2]. In most cases, a wireless sensor network will be composed of a large number of densely deployed sensor nodes. Neighboring nodes might be very close to one another, resulting in high interference and power-consumption levels. Furthermore, one of the most important

 ISSN 1045-9243/2012/$26 ©2012 IEEE

constraints of sensor nodes stems from their limited – generally, irreplaceable – power sources. Therefore, while traditional networks aim at achieving high quality of service (QoS) provisions, wireless-sensor-network protocols must focus primarily on power conservation. Tradeoff mechanisms seem necessary to increase reliability at the cost of lower throughput or higher latency. An essential design issue is related to the investigation of system parameters, such as network size and node density, with regards to system metrics including spatial coverage, throughput, latency, network lifetime, energy efficiency, and reliability, and how these affect the tradeoffs previously mentioned.

These issues have been engaged in the literature, with most approaches having focused on routing optimization and protocol design. Many researchers have developed schemes that fulfill the requirements described above, proposing protocols and algorithms for wireless sensor networks. Quality of service can be measured in terms of energy efficiency, or the optimum number of sensors sending information at any given time [7, 8]. In the latter case, quality-of-service control mechanisms, built on the Gur Game Paradigm, have been put forward to adjust quality-of-service resolution, thus extending network lifetime and managing energy depletion. Later, J. Frolik [9] extended the Gur game approach, and, additionally, illustrated a second method providing quality-of-service feedback through packet acknowledgments. Apart from the introduction of new MAC-layer protocols (QUality-of-service-specific Information REtrieval (QUIRE)) [10], Z-MAC [11], i-GAME [12]), and network-layer protocols, e.g., MMSPEED [13], cross-layer design [14] is a novel approach that has lately come under close scrutiny.

Minimizing node interference is undoubtedly one of the main challenges in wireless sensor networks. High interference increases the packet-collision probability, which, in turn, affects efficiency and energy consumption. Early approaches focused on reducing the node degree [15, 16]. Topology control mechanisms inspired by graph theory have been developed to conserve energy in wireless sensor networks without being able to explicitly guarantee low interference. Some examples include the work of Burkhart et al., using a minimum spanning tree (MST) [17]; the highway model, proposed by Rickenbach et al. [18]; and the "Minimizing Interference in Sensor Network (MI-S)" algorithm introduced by A. K. Sharma et al. [19]. In addition, Jang [20] drew inspiration from graph theory to propose geometric algorithms, reducing interference based on the conversion of network problems to geometry problems. Last, J. Tang et al. [21] studied multi-channel assignments to achieve interference-aware topology control in wireless mesh networks.

On the other hand, smart antennas have been extensively used in the literature of more conventional communications systems, and their usage is likely to expand more, due to their proven beneficial impact in wireless communications performance [22]. Smart antennas have been suggested in order to satisfy the demand for spontaneously high data rates to certain users, while maintaining a high level of quality of service for conventional users [23]. They have been also used in order to mitigate interference and delay spread, increase system capacity and spectral efficiency, combat multipath fading, address the near-far effect, and increase cell coverage [24, 25]. Furthermore, they have been suggested for radiation-pattern diversity, space-division multiple access, direction-of-arrival estimation and localization, etc. [26-28].

Herein, it is proposed that wireless-sensor-network nodes be equipped with smart antennas. It is also proposed that certain slight changes be implemented in the node-selection and routing processes, in order to address the inherent drawbacks of such networks with an efficient tool, only this time in the physical layer. Our aim is to analyze a novel technique for overcoming the limitations arising from sensor nodes. We also attempt an investigation into pertaining design constraints promoting the use of certain tools to attain our main objectives. The emergence of adaptive systems, such as smart antennas, can boost the performance of wireless sensor networks aimed at satisfying the growing demand for robust infrastructures. To the best of our knowledge, the incorporation of smart antennas in wireless-sensor-network nodes – either as-is or together with node selection and routing modifications – has not been reported in the literature.

The remainder of this paper is organized as follows. In Section 2, the simulated wireless-sensor-network model is established, with the network setup, its operating modes, and the basic transmission mechanism. Section 3 demonstrates the improved network performance evaluated in terms of quality of service, efficiency, and node activity. Section 4 considers energy consumption associated with the studied modes. Section 5 offers a performance comparison among smart-antenna modes with an increased number of beams (Section 5.1), or among wireless sensor networks with mixed smart and omnidirectional nodes (Section 5.2). Finally, Section 6 concludes the paper.

2. WSN Model and Formulation

This section provides an overview of the proposed approach and the general framework upon which the simulation is based, along with the principal assumptions associated with our modeling. Furthermore, the basic mechanisms that define the network operation are introduced. Hereinafter, it is assumed that the operating-frequency band of the presented wireless sensor networks is the 2.4 GHz ISM band, complying with the 802.15.4 IEEE standard.

2.1 Network Setup

Smart antennas can substitute for omnidirectional antennas at wireless-sensor-network nodes. This is because they can transmit within the total coverage area of an omnidirectional antenna, yet with a directional gain that depends on the beam activated at each time slot. This means that the relative angular position of the pair of source and destination nodes will determine the beam that will be activated for each node, serving for either transmission or reception. This way, a well-defined area with locally specified bounds is considered busy for each ongoing transmission, and every node within this range is rendered incapable of transmitting data. In other words, the utilization of beams can actually reduce the interference, and limit the collision area to narrower sectors instead of full discs of the same radii, as in the case of omnidirectional antennas. However, the gain will differ with angle, since it will generally depend on the actual angle between source-destination nodes.

Different network topologies are examined in this work. Each one is characterized by a different node density, node-deployment mode, and, essentially, the way nodes are linked. The latter is reflected in the adjacency matrix, which is essentially a record of the various node pairs within the network that are within communication range of each other. The adjacency matrix is generated as follows. For each pair of nodes, e.g., n_1 and n_2, we compute the receiving power of the second node (n_2) with the first node considered to be the transmitting node. The receiving power is herein calculated by the Friis equation:

$$P_{rec} = P_t \frac{G_1 G_2}{L}\left(\frac{\lambda}{4\pi d}\right)^2, \qquad (1)$$

where P_{rec} represents the received power, P_t represents the transmitted power, G_1 represents the transmission gain of node n_1, G_2 represents the receiving gain of node n_2, L represents the propagation losses, λ represents the wavelength, and d represents the distance between n_1 and n_2.

At the receiver's side, a power threshold determines whether it can successfully accept the transmitted signal, i.e., whether $P_{rec} > P_{rthres}$. In this case, a directional link pointing from n_1 to n_2 is added in the adjacency matrix, denoted by a one at the element $[n_1, n_2]$. Otherwise, there is no direct connection from n_1 to n_2, and this element of the adjacency matrix has a zero value.

Upon network-simulation setup, we need to specify the value of the maximum gain of each beam with respect to the omnidirectional gain, so that the networks generated are comparable in terms of link density. We thus assume that the gain of omnidirectional antennas equals 3 dB, which is a popular gain for commercial ISM antennas. The maximum value of each of the beams is approximately doubled, which is a reasonable assumption for an array of four commercial elements [29-31]. This means that $G_i = 2\times10^{0.3} = 4$, or, equivalently, 6 dB. This serves to maintain a 3 dB gain that is close to the gain of the omnidirectional antennas, thus achieving similar connectivity patterns throughout the network. The radiation pattern of each node is shown in Figure 1.

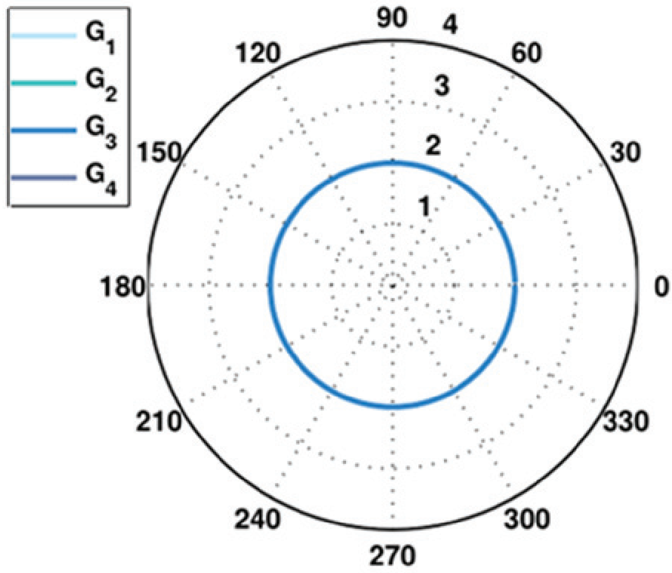

Figure 1a. The radiation patterns of an omnidirectional antenna.

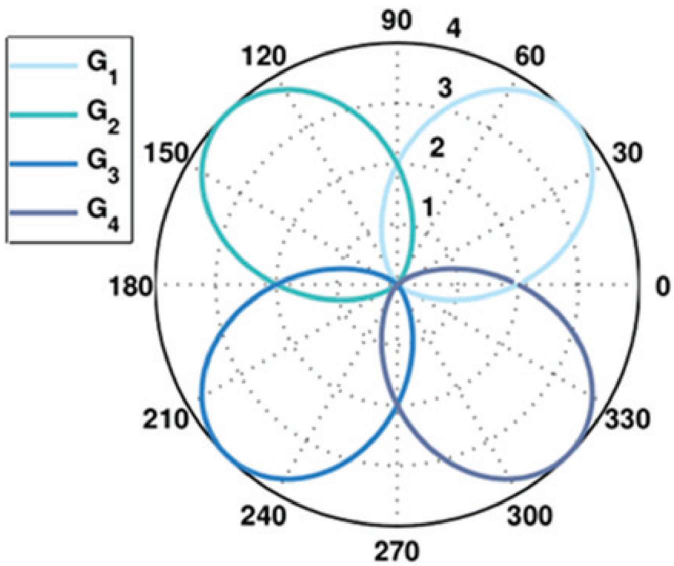

Figure 1b. The radiation pattern of a four-beam smart antenna.

2.2 Network Operating Modes

In this section, we compare the different modes in which networks operate. First, we deploy a number of nodes, e.g., $N = 25$, within a deployment area of size 50 × 50 m^2, and build the adjacency matrices for each operating mode (nodes are uniformly distributed in the deployment region). We assume that the area is free of impediments, with propagation losses of 6 dB. The frequency is set to 2.4 GHz, the transmission rate is

1 Mbps, while the receiver's sensitivity approximates −100 dBm. In addition, we need to adjust the number of time slots, which will enable us to evaluate the performance of each network type based on the same merit. It should be noted herein that carrier-sense multiple access with collision avoidance (CSMA-CA) is assumed for the presented wireless sensor networks; hence, a node cannot transmit/receive to/from more than one node at the same time.

2.2.1 Omnidirectional Antennas Operating Mode

In this mode, nodes are devices equipped with omnidirectional antennas. In this mode, the gain of the transmitter and receiver are equal to each other, i.e., $G_1 = G_2$: thus, every link becomes reciprocal.

2.2.2 Smart Antennas Operating Mode

In this mode, nodes are equipped with smart antennas. In this mode, $G_1 \neq G_2$. In order to compute Equation (1), we need to find the angle between n_1 and n_2. For this angle, we next find the beam that is going to be activated for each node when n_1 is the transmitter and n_2 is the receiver, so as to compute the transmitting and the receiving gains, accordingly. Lastly, we examine whether the receiving power is above or below the threshold (the receiver's sensitivity), and we either add a link in the adjacency matrix or we do not.

The main difference between these two modes lies in the configuration of the collision areas, i.e., the sectors occupied by active transmissions. A model for calculating these areas will be provided later herein (Section 2.6).

Figure 2 shows the way nodes interfere with each other and form coverage areas while attempting transmission. In Figure 1, the common coverage area is defined as the intersection of the discs, while their union defines the blockage area, in which every other node is unable to transmit. Figure 2 shows the total coverage area during an ongoing transmission between nodes n_1 and n_2 when they use smart antennas, and, consequently, only one of the four beams is activated. It becomes clear that total interference is significantly reduced, a smaller number of nodes are blocked, and more free space becomes available for the nodes remaining inactive in the network. Figure 1 shows a different example, where node n_1 does not transmit towards n_2, but instead node n_1 exchanges information with another node within the sector covered by its activated beam (steered towards the left). Although these two nodes are able to communicate with each other, they do not block each other when communicating with other nodes: this would not be the case for the omnidirectional-antennas mode. In Figure 1, n_2 remains always within the range of n_1, and is thus excluded from transmitting on the condition that n_1 is currently sending data to a third node.

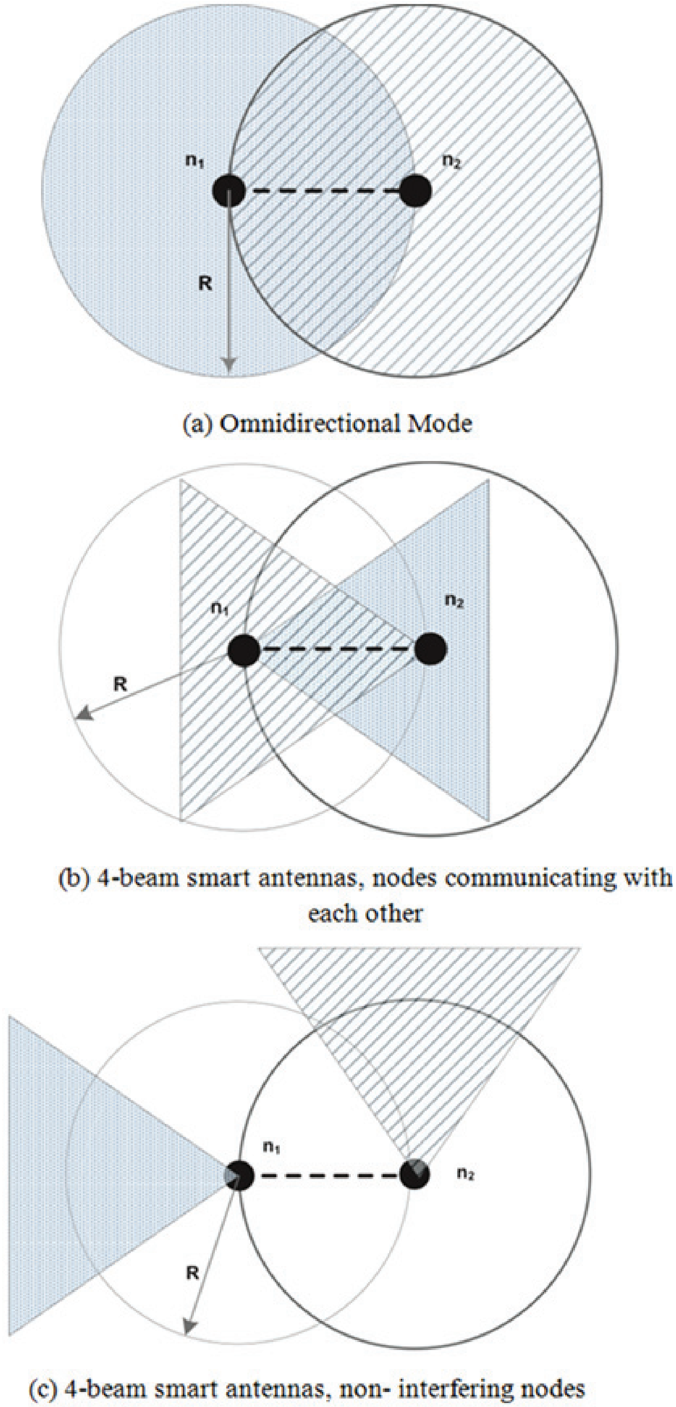

Figure 2. The interference between active nodes: (a) omnidirectional mode; (b) four-beam smart antennas, with the nodes communicating with each other; (c) four-beam smart antennas with non-interfering nodes.

2.3 Simulation Algorithm

Apart from the way nodes get connected in the network, we need to clarify how the procedure takes place. Consequently, at each time slot:

1. For every single node, packet generation follows the Poisson distribution, with parameter λ. Packets

with the same identity number (id) comprise the same message, which has a unique destination, source, transmission time, and success field (updated only if the packet reaches its final destination within the simulation time). It is worth noting that a message might contain more than one packet, as it represents the total amount of information generated at the source aimed at being delivered to the desired destination.

2. Each node that has data to send senses the wireless medium, and attempts transmission in the case where it is not blocked by another transmission. No priority scheme is set and transmitting nodes are selected randomly, as in a realistic case where nodes are not centrally controlled when trying to sense the medium and initiate transmission.

3. The queues at each node operate on a first-in first-out order. The first packet in the queue is picked, and, after determining its destination, the shortest path is computed according to Dijkstra's algorithm [34]. For this particular path, if the next-hop node is busy, the packet stays in the current node's queue until it can be retransmitted; otherwise, it is transmitted to the next node and is removed from the current node's queue. The average number of hops (average path length) and the total time from source to destination can provide a rough estimate of the average time spent at each intermediate node.

4. The pair of nodes that is currently exchanging data does not allow other nodes within the same range to start transmitting. These nodes are disabled and cannot transmit at the same time slot.

2.4 Definitions and Assumptions

A list of definitions and assumptions follows herein, in order to put the numerical results into the right context:

1. The number of execution steps stands for the number of time slots. We speed up convergence by prohibiting packet generation from a pre-determined simulation step and onwards. However, the number of time slots that is considered sufficient to reach a desirable steady state, and thus avoid overflows in node queues, needs to be determined. After simulating the same network for various parameter values with the number of time slots ranging from 100 to 5000, we concluded that the fluctuations can be considered negligible, since the performance-metric results varied only slightly as the number of time slots increased (Figure 3), i.e., they practically remained unaffected. Hence, the number of time slots does not necessarily have to be too large in order for the results to be indicative of the network performance. Therefore, we set a moderate number of time slots equal to 1000, since our aim was to check the efficiency of the network when it operated under normal circumstances, as usual. We thus are able to compare the different operating modes, and the improvements the networks are due to the installation of smart antennas on the nodes.

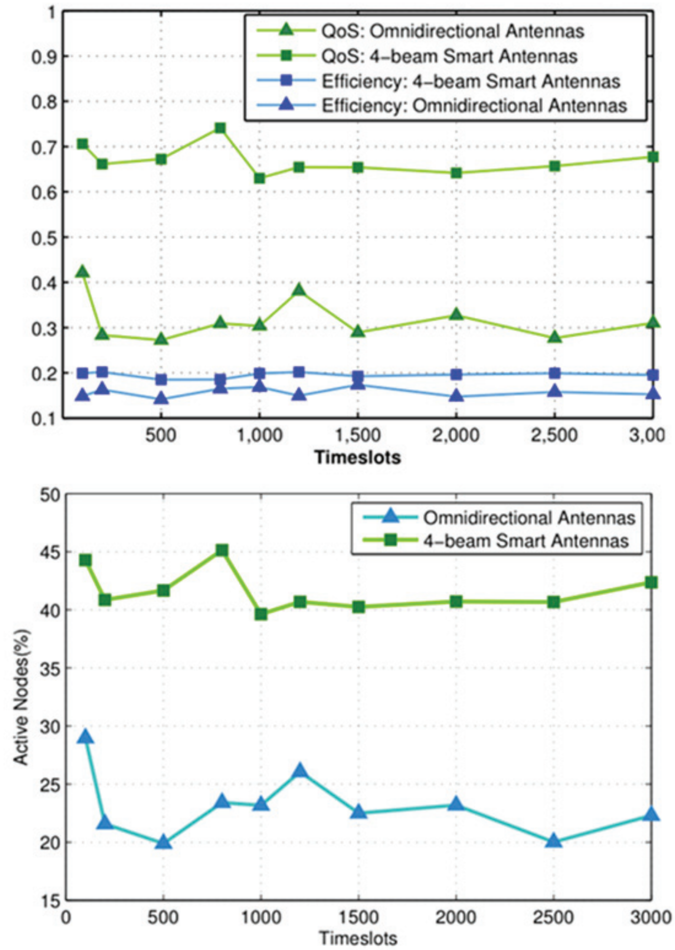

Figure 3. The simulated fluctuations in the performance metrics with respect to simulation time slots (node density: $1/100\ \text{m}^2$, $\lambda = 0.5$).

2. The nodes for which the queue is not empty, i.e., for which there is available information to be sent, attempt transmissions at most once during each time slot. We assume that the MAC protocol used is CSMA/CA, which means that transmitters avoid transmission whenever they detect ongoing traffic, and keep the packets in their queue until the next time slot. The collision areas are determined in the way previously described (the areas specified by the sectors of the pair of beams). When their queues are full, they drop the packets: this case is translated as packet loss (failure).

2.5 Basic Network Metrics and Parameters

In order to evaluate network performance, we consider the following performance metrics:

Quality of Service (QoS): the ratio of the number of packets the transmission of which has commenced to the total number of packets that have been generated (total network load).

Efficiency: the ratio of the number of messages successfully delivered from source to destination, to the total network load generated throughout the simulation.

Percentage of active nodes, a (%): the average number of nodes allowed to transmit within the same time slot without being blocked due to interference caused by ongoing network traffic. A small percentage of active nodes corresponds to more collisions, which reduces network efficiency.

Furthermore, the above are considered with respect to the following set of parameters:

- Node density (nodes per square meter)
- Poisson parameter, λ
- Transmitted power, P_t

As far as node density is concerned, it is – by definition – the ratio of the number of nodes deployed within the network region to the total deployment area. The parameter λ determines the rate at which packets are generated during each time slot. We should take care of the maximum value this parameter can take, given that if we let the number of packets arbitrarily increase and at a high rate, the results will not be representative of the network's performance. Finally, by transmitted power we refer to the transmitted power of each node, which goes for the whole network, since we assume that the network is homogeneous, i.e., each node displays identical features.

2.6 Collision Areas, Probability of Transmission, and Energy Consumption

We now present a mathematical analysis of the collision areas and the transmission probability, based on the mechanisms described in Section 2. In Figure 4, A_n denotes the coverage area of node n. For instance, let as assume that we place one node approximately every 10 m: the mean distance between each pair is then 10 m. We could alternatively compute the maximum radius, R, using the Friis Equation and setting $P_{rec} = P_{rthres}$. Assuming that R is known, we can analytically calculate the collision areas. Defining the collision areas of nodes n_1, n_2 by A_{n_1} and A_{n_2}, as well as the source-destination pair's common area by A_{n_1,n_2}, it can be easily deduced that in the omnidirectional mode, it holds that $A_{n_1} = A_{n_2} = piR^2$, i.e., A_{n_1} and A_{n_2} correspond to the areas covered by a full disk. Furthermore, their common coverage area, A_{n_1,n_2}, has been calculated [33], and is given by $4\int_{\frac{d}{2}}^{R}\sqrt{R^2-x^2}\,dx$ (see Figure 4).

Regarding the smart-antennas mode, the coverage areas are defined as the sectors covered by each node's transmission range. For simplicity, it is assumed that this area corresponds to $1/N$ of the area covered by full discs, where N denotes the number of beams available by the smart antenna. In the case of a smart antenna with four beams, like the one in Figure 1a, this is equal to one-quarter of the area of full discs, i.e., $\frac{1}{4}\pi R^2$. As for the source-destination pairs' common area, this varies since it is a function of the actual angle between them. Here, we can make the assumption that the antennas are optimally oriented, hence the value of their common area, A_{n_1,n_2}, is equal to the area in the previous case, i.e., $4\int_{\frac{d}{2}}^{R}\sqrt{R^2-x^2}\,dx$, since this area is the intersection of the radiation patterns of the pair of nodes as they were presented in Figure 4. It should be noted herein that the coverage area of a node defines a collision area. Therefore, as far as the performance of the smart-antenna mode is concerned, the assumptions in this paragraph configure a worst-case scenario. This is because the arising coverage areas are always larger than the actual areas corresponding to real smart-antenna systems.

We estimate the probability of transmission for a single node. This occurs as the probability of the node being selected earlier than its neighbors, which means that it is not in a disabled state due to ongoing transmissions.

The transmitting probability, P_t, of a single node, i, is given by Equation (2):

$$P_t(i) = p_n(i)\left(1-\frac{n}{N}\right)^{nodeDegree(i,\mu)}. \qquad (2)$$

Proof. Let p be the probability that a node i is the *n*th node to be selected within a specific time slot, which is a random event, and thus $p_n(i) = \frac{1}{N}$. The probability q that a node j has not yet been selected within the same time slot is one minus the union of the following possibilities: it was selected first (let us define it as P_1), second (P_2), ..., or *n*th (P_n). These events are mutually exclusive since they obviously do not occur simultaneously. This yields

$$\begin{aligned} q_n(j) &= 1-\left(P_1 \cup P_2 \cup \ldots \cup P_n\right) \\ &= 1-\left[p_1(j)+p_2(j)+\ldots+p_n(j)\right] \\ &= 1-\left(\frac{1}{N}+\frac{1}{N}+\ldots+\frac{1}{N}\right) \\ &= 1-\frac{n}{N}. \end{aligned}$$

The probability that a node does not interfere with its neighbors, implying that neither of the neighbors has been selected so far, is the intersection of the events that the neighbors have not yet been selected. Those events are independent, since the occurrence of one event does not interfere with the other events, i.e., their intersection comes as the product of the single probabilities:

$$\bigcap_{allnodesj;l_{ij}\in E} q_n\left(j\right)=\prod_{allnodesj;l_{ij}\in E}\left(1-\frac{n}{N}\right)=\left(1-\frac{n}{N}\right)^{nodeDegree(i,\mu)} \quad (3)$$

The transmission probability for node i is thus defined as the combined probability that the node is selected nth ($p_n\left(i\right)$) and is not blocked by neighboring nodes (Equation (3)):

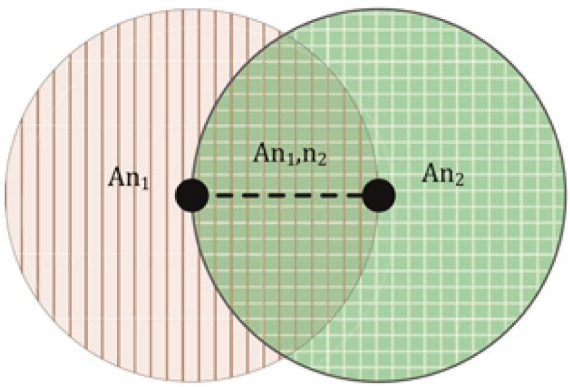

Figure 4a. The calculation of the collision area ($A_{n_1}+A_{n_2}-A_{n_1,n_2}$) for the omnidirectional mode: $A_{n_1}=A_{n_2}=\pi R^2$, $A_{n_1,n_2}=4\int_{\frac{d}{2}}^{R}\sqrt{R^2-x^2}\,dx$.

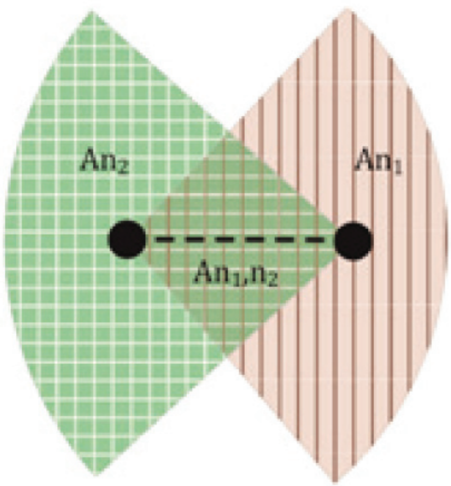

Figure 4b. The calculation of the collision area ($A_{n_1}+A_{n_2}-A_{n_1,n_2}$) for the four-beam smart-antennas mode: $A_{n_1}=A_{n_2}=\pi R^2/4$; A_{n_1,n_2} varies.

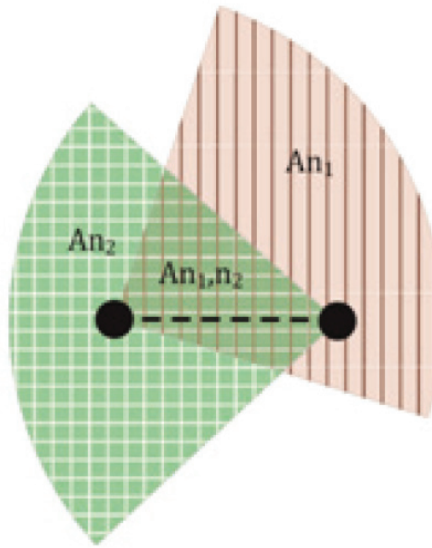

Figure 4c. The calculation of the collision area ($A_{n_1}+A_{n_2}-A_{n_1,n_2}$) for another four-beam smart-antennas mode: $A_{n_1}=A_{n_2}=\pi R^2/4$; A_{n_1,n_2} varies.

$$P_t\left(i\right)=p_n\left(i\right)\left(1-\frac{n}{N}\right)^{nodeDegree(i,\mu)},$$

where $nodeDegree(i,\mu)$ is the degree of node i when the network operates on mode μ , with values 0 and 1, holding for omnidirectional and smart antennas, respectively .

As for $nodeDegree(i,\mu)$, i.e., the number of nodes $j \mid l_{ij}\in\left|E\right|$, where $\left|E\right|$ is the set of the edges of the graph, this is explicitly computed using spatial analysis, i.e., techniques based on analytic approaches to study topological and geometric properties, since we have assumed uniformly distributed nodes within the total coverage area. A uniform node distribution implies that since the number of nodes within the total region of L^2 square meters is N , the number of nodes within an area of A square meters is expected to be $\frac{A}{L^2}N$. The average node degree, i.e., a node's neighbors, is thus easily computed when its coverage area is known. Considering this analysis in association with Figure 4, showing the area covered by a single node in the two different operating modes, it follows that

$$nodeDegree\left(i,\mu\right)$$
$$=nodeDegree\left(\mu\right)=\begin{cases}\frac{\pi R^2}{L^2}N=\pi R^2\rho,\ \mu=0\\ \frac{\pi R^2}{4L^2}N=\frac{1}{4}\pi R^2\rho,\ \mu=1\end{cases}. \quad (4)$$

The numerator is the coverage area of node i as described in Figure 4 and has a fixed value regardless of node i , since we have assumed that nodes have equal transmitted power and, therefore, the same transmission range, R. This explains why we substituted $nodeDegree(\mu)$ for $nodeDegree(i,\mu)$. We also set N/L^2 as the node density, defined as ρ.

From Equation (2) it is obtained that the higher the node degree, the smaller the possibility of transmission. It also becomes evident that node degree depends exclusively on the μ parameter. This makes it clear that the average node degree for the network is equal to each individual node's degree. Besides this, the dependence of a node's degree on the μ parameter indicates the superiority of smart antennas over omnidirectional antennas. When smart antennas are used, the node degree is modified with respect to the activated beam: in the omnidirectional mode, the node degree remains fixed, and exhibits a fourfold increase compared to the smart-antennas mode, which is verified by Equation (4). Each transmitting node induces the deactivation of its neighbors, or, in other words, for every single node i, $nodeDegree(\mu)$ nodes are blocked. Defining the percentage of active nodes as $A[\%]$, it holds that

$$\frac{A}{100}N + \frac{A}{100}N\,nodeDegree(\mu) = N\,,$$
$$A[\%] = \frac{100}{1+nodeDegree(\mu)}\,, \tag{5}$$

i.e., the number of nodes equals the number of active nodes and the number of the nodes blocked owing to active nodes. Substituting the values for each operating mode, the active-nodes percentage is computed from Equation (6):

$$A[\%] = \begin{cases} \dfrac{100}{1+\dfrac{\pi R^2}{L^2}N}, & \mu = 0 \\ \dfrac{100}{1+\dfrac{\pi R^2}{4L^2}N}, & \mu = 1 \end{cases} . \tag{2.6}$$

Following the previous analysis, energy consumption can be estimated both for individual nodes and for the entire network, taking into account the percentage of active nodes, $A[\%]$, and their transmitted power. More specifically, the number of active nodes multiplied by the average transmitted power is the energy consumption of the active nodes. Assuming that the rest of the nodes remain idle, the corresponding energy consumption is given by the number of idle nodes multiplied by the idle-state consumption rate. Representing the consumption rate by $a[\%]$ and the rate at which energy is depleted at the idle state by $\gamma[\%]$, it follows that at time step t:

$$E(t) = A\,E(t-1)\frac{a}{100} + (1-A)E(t-1)\frac{\gamma}{100}\,, \tag{7}$$

where $E(t)$ and $E(t-1)$ correspond to the total available energies at time t and $t-1$, respectively, while A denotes the number of active nodes.

2.7 Network Topology

Network topology and the way operating modes are differentiated may be better explained through a graphical example (Figure 5). A network model and its state after adding the links is presented, first having nodes transmitting omnidirectionally (Figure 5a), and then using smart antennas (Figure 5b). The difference lies in the number of links added, making the nodes equipped with smart antennas able to communicate over greater distances, since the gain is higher towards every direction. This explains why the graph becomes denser with regard to its set of edges when it operates in the smart-antennas mode.

All numerical results presented in the following sections were calculated by averaging the corresponding network metrics for a large number (more than 100) of random topologies like those shown in Figure 5. This aided towards proving the validity of our conclusions, and contributed to the successful evaluation of the performance of both network operating modes.

3. Evaluation of Metrics with Respect to Network Parameters

In this section, we present certain numerical results of the network simulation. Our analysis was performed as functions of node density and the parameter λ, while taking into account the following system metrics: quality of service (QoS), efficiency, and percentage of active nodes.

3.1 Node Density

Node density plays a vital role in network efficiency, as it constitutes a determining factor for both the collision areas and the shortest paths used in information dissemination. As node density increases, more nodes lie in the same sectors, and are disabled due to ongoing transmissions. As will be demonstrated by the numerical results, sparse networks did not demonstrate significant improvement after installing smart antennas, while the opposite phenomenon was observed for denser networks. The collisions detected were fewer, but as the network increased in size, the link density increased at a high rate, thus impeding successful transmissions without collisions. The problem got worse when nodes used omnidirectional antennas.

Initially, we assumed that the network covered a square region with an area equal to 50 m × 50 m. In this area, we deployed a fixed number of nodes. We thus started from placing one node every 15 m, which corresponded to a node density

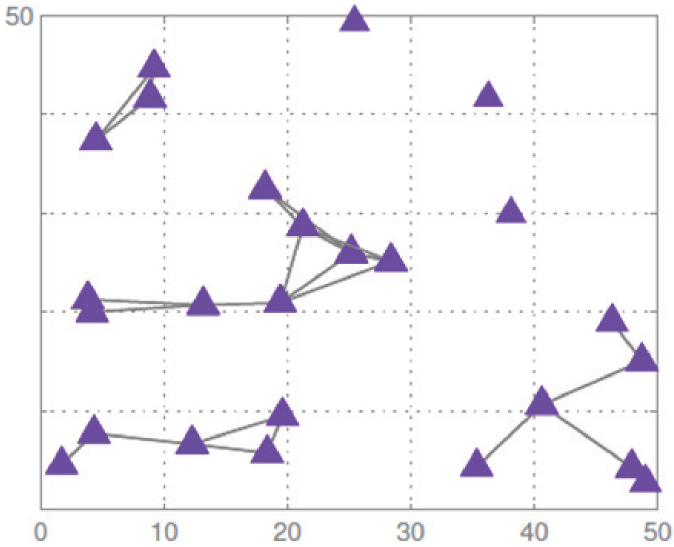

Figure 5a. The network topology and node links for the omnidirectional mode (grid size: 50 m × 50 m).

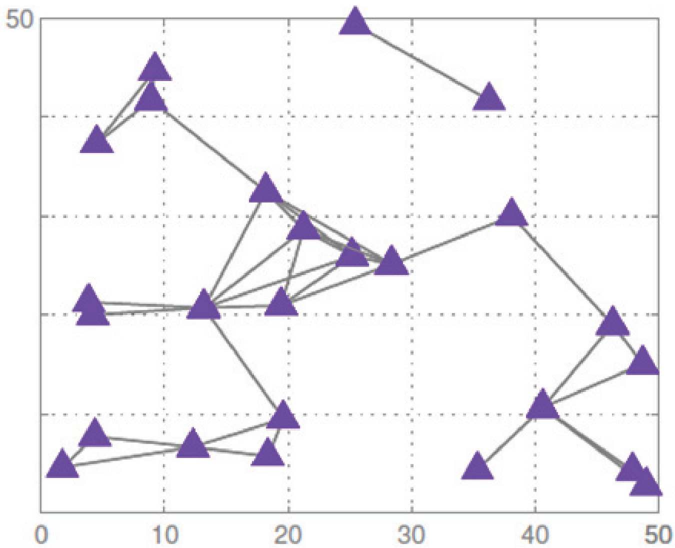

Figure 5b. The network topology and node links for the smart-antennas mode (grid size: 50 m × 50 m).

of 0.005 nodes per square meter. We then gradually increased the number of nodes deployed until there existed approximately one node every 6 m (in this case, the node density was 0.025). As illustrated in Figure 6a, the quality of service was improved as the network became denser. This was mainly due to the lack of connectedness that appeared in more-sparse networks. However, this parameter tended to converge to a constant value as the node density rose over 0.015 nodes per square meter. The improvement of the quality of service with smart antennas over omnidirectional antennas was approximately 20% at almost every density value. This was a considerable difference, since more transmissions were activated within the same time period. It should be noted that the low quality of service of the fourth point for the omnidirectional case in Figure 6a was due to a slight averaging fluctuation, and did not cancel the discussed trends.

Furthermore, we discuss how efficiency is influenced by node density. It is noteworthy that when omnidirectional antennas were used, the network's efficiency both significantly and rapidly dropped as the node density increased. Initially, as long as the network was sparse, the achieved efficiency was high. However, sparse networks – inducing low link density and, consecutively, low interference – were not within our areas of interest, given that conventional wireless sensor networks need to be connected. By this, it is meant that the phenomenon of the existence of isolated nodes had to be eliminated. This was secured for density values above 0.015. On the other hand, networks using smart antennas diverged from this behavior, and showed a tendency to keep efficiency rates at the same levels. In other words, they guaranteed that most packets would be successfully delivered to the destination, mainly due to decreased interference levels.

Finally, there was a performance improvement regarding active nodes, as illustrated in Figure 6, since the percentage of active nodes was always higher compared to the omnidirectional mode. This difference ranged from 10% and rose up to 20% of the total number of nodes, N; this percentage corresponded to five to 10 more active nodes when $N = 50$, 10 to 20 when $N = 100$, etc.

Finally, for completeness, we included numerical results for the case where it was assumed that the maximum gain of each beam was equal to the gain of the omnidirectional mode (Figure 7). The trend of network performance with respect to node density for both the omnidirectional and smart-antenna modes was the same as in Figure 6. Nevertheless, it should be pointed out that the comparison between an omnidirectional and a smart-antenna-equipped node was unfair, and favored the former. This was due to the inherently increased link density of omnidirectional nodes compared to smart-antenna nodes, even in the case of equal node-density values. More specifically, as analyzed in Section 2, the links of a smart-antenna node are sparser towards angles different from that of the main beam, due to gain reduction *D*, especially towards the edges, as well as out of the beams. Nonetheless, Figure 7 illustrated that smart-antenna-equipped nodes exhibited a performance that was similar to that of omnidirectional nodes. Moreover, as the node density increased, the performance of the former became superior to that of the latter, and this trend kept on for larger node-density values. It is understood that as long as the node density reaches a threshold value of sufficient connectedness, the lower interference levels associated with directional antennas overcome the disadvantage of lower link density, and the performance of the respective nodes is boosted.

3.2 Parameter λ

The performance of each operating mode with respect to the Poisson parameter, λ, was examined. The λ parameter essentially reflects the network's traffic. For example, a busy network where information continuously flows exhibits a large value of λ, and tends to display undesirable behavior when queues overflow. On the other hand, networks in which infor-

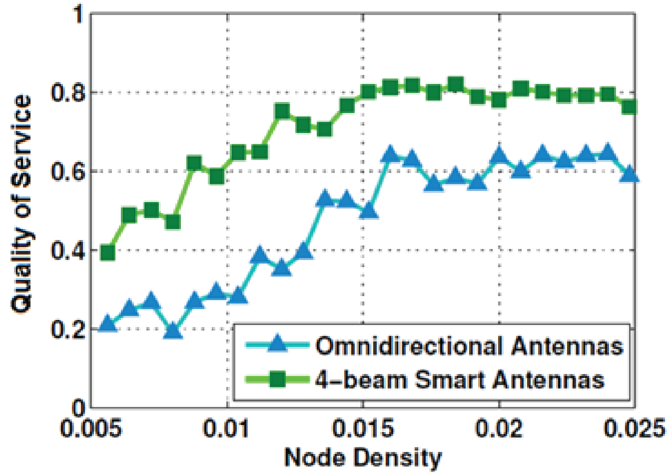

(a) Quality Of Service

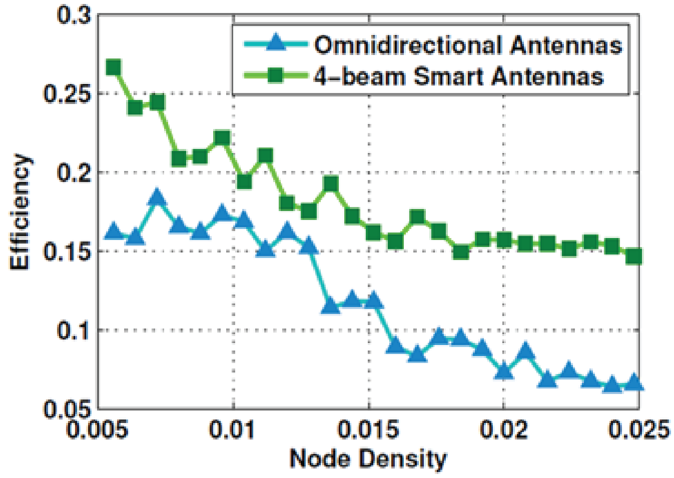

(b) Efficiency

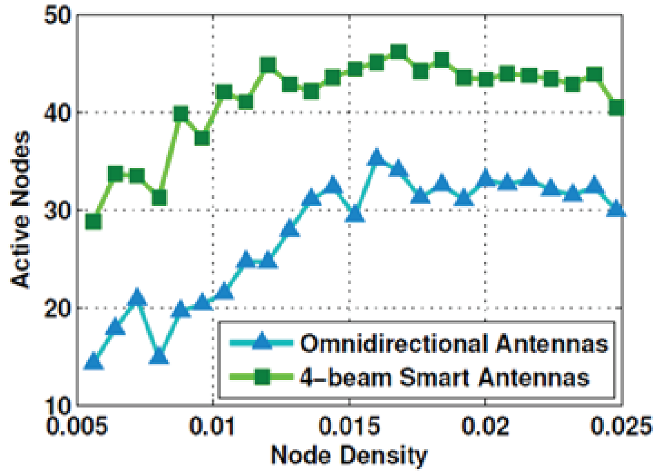

(c) Active Nodes

Figure 6. The network performance with respect to the node density, $\lambda = 0.5$: (a) quality of service; (b) efficiency; (c) active nodes.

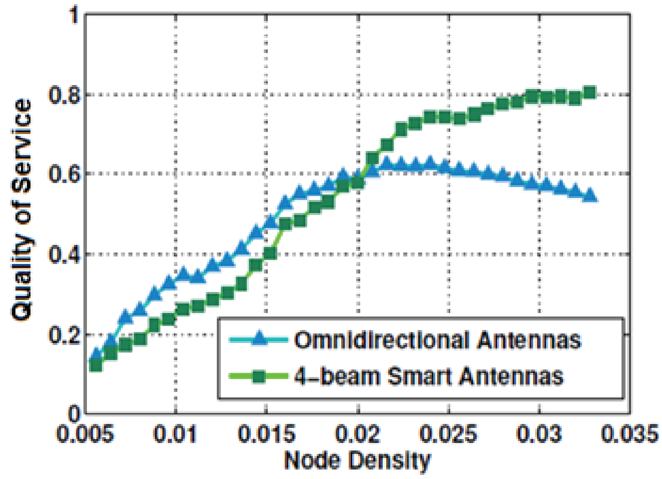

(a) Quality Of Service

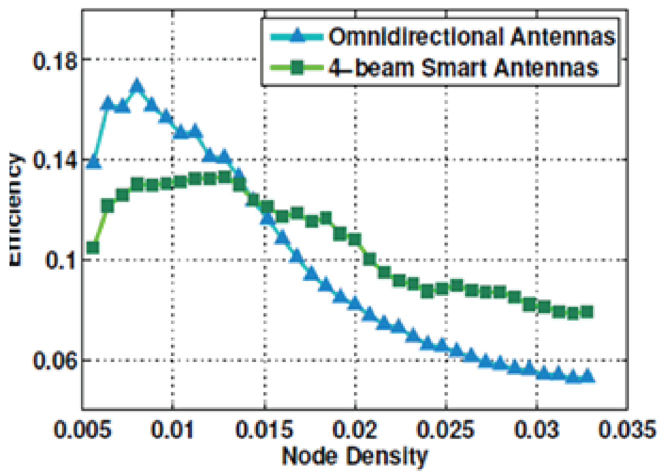

(b) Efficiency

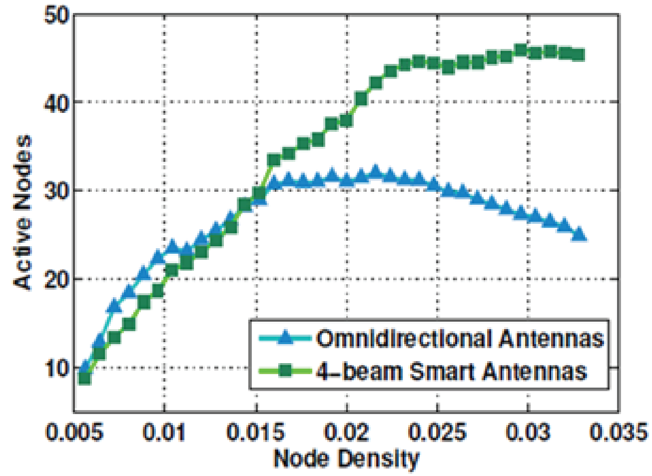

(c) Active Nodes

Figure 7. The network performance with respect to the node density assuming constant gain, $\lambda = 0.5$: (a) quality of service; (b) efficiency; (c) active nodes.

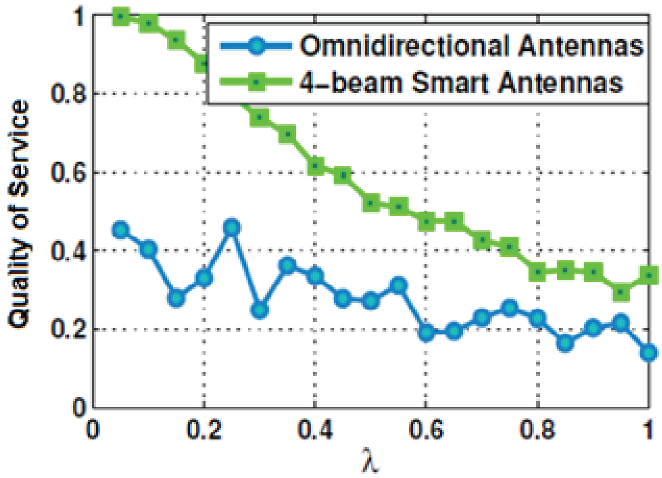

(a) Quality Of Service

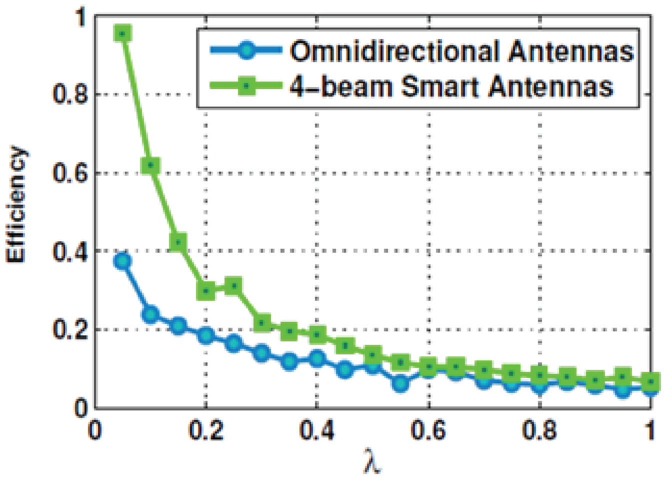

(b) Efficiency

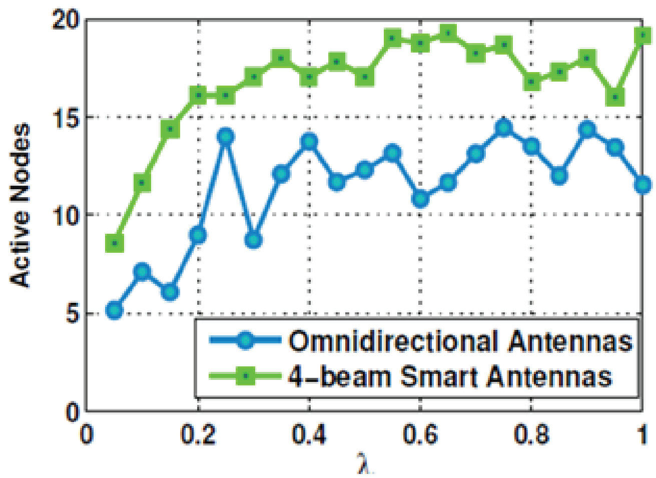

(c) Active Nodes

Figure 8. The network performance with respect to λ, for a node density of one node per 100 m^2: (a) quality of service; (b) efficiency; (c) active nodes.

mation steadily flows and at lower rates tend to provide a better quality of service and be far more efficient, compared to the previous case. We thus needed to study the network's performance under different network-traffic conditions.

Figure 8 demonstrates the way the parameter λ affected the network's performance for both operating modes. As this parameter increased, performance deteriorated for both operating modes. Smart antennas displayed a sharper decrease, mainly due to the high values achieved when the information was generated at lower rates. Nevertheless, the performance of smart-antenna wireless sensor networks was always better compared to omnidirectional wireless sensor networks. More specifically, the quality of service and the efficiency took a value of one as long as the network traffic remained low, while they dropped significantly as packets were generated at higher rates.

Furthermore, as far as the percentage of active nodes was concerned, the smart-antenna mode always delivered higher performance, which steadily increased with increasing values of the parameter λ. This was expected, since on the one hand, the interference levels increased in the omnidirectional mode since almost every node had packets to send, and most of them blocked the nodes they were connected with. Besides that, the high packet-generation rate did not affect both modes to the same degree: the smart-antenna mode was less affected, in that more nodes were able to transmit, due to the smaller coverage areas formed and the smaller number of nodes blocked. The percentage of active nodes also increased with parameter λ as expected. A node could be active only when it transmitted data, which presupposed that packets were generated within its queue. When λ was low, most node queues were empty, and the ongoing activity was small. This situation inverted as λ increased. We did not consider greater values (e.g., $\lambda > 1$), since in that case, the queues would most likely have overflowed, thus not allowing for fair evaluation of the operating modes.

It should be also noted that the peaks at the fifth point for the omnidirectional case of both Figures 6a and 6c were due to slight averaging fluctuations, and did not affect the discussed conclusions.

4. Energy Consumption

This section is dedicated to one of the most important factors for wireless sensor networks. Energy consumption plays a key role in the network's operation, and should be taken into consideration upon designing and manufacturing wireless nodes and sensors. Under the condition that every node has the same energy capabilities – i.e., energy reservoirs, transmitted power, energy depletion time, energy-consumption rate, etc. – we can easily deduce that a decrease in the transmitted power can affect all the rest of the energy determinants. This decrease is herein achieved by increasing directionality via the use of smart antennas. Since the distances between each pair of nodes are known in advance, we can have the nodes accordingly adjust their transmitted power. Instead of increasing the number of links of the networks produced by keeping the transmitted power fixed, we thus modified our simulation plan by reducing the transmitted power of nodes equipped with smart antennas. This approach was considered to be more "fair" when comparing smart-antenna nodes with omnidirectional nodes. Later in this section, we examine the possibility of adjusting the transmitted power of each node with regard to the global threshold value. Despite this being a costly solution, it can improve network efficiency by simultaneously reducing interference and energy consumption.

Given that the transmitted power for networks operating in the omnidirectional mode was fixed, we studied the behavior of networks with smart antennas, and examined lower values of transmitted power for different network topologies. Hence, we could draw conclusions about the point where throughputs were equalized, and the amount of energy saved after the evaluation period. Let us elaborate on Figure 9, where parameter a corresponded to a fraction of the initial transmitted power, the value of which was universal in the network (given that the network was considered a homogeneous network, every node having the same transmitted power capability). The transmitted power in the omnidirectional mode was 10 mW, and the cases evaluated included networks using smart antennas with reduced power (ranging from 10 W where $a = 100\%$, to 2.5 mW corresponding to $a = 25\%$), reflected by the a parameter. As expected, the most efficient network corresponded to $a = 100\%$. However, the point where the quality of service with smart-antenna nodes remained at the same levels compared with omnidirectional nodes corresponded to a much lower transmitted power, which equaled 75% of its initial value (i.e., with omnidirectional nodes). This was somewhat expected, but the energy conservation was spectacular. Due to the higher gains of each beam of the smart antennas, high transmitted power led to a greater number of links, and therefore higher levels of interference. By reducing transmitted power, we achieved the following:

- The quality of service was approximately equal to the level achieved when nodes transmitted with the maximum power. Approximately the same number of packets were thus being serviced in the same time period.

- The percentage of active nodes within the same time slot was greater by almost 2%, compared to the case of $a = 100\%$ of P_t, and was almost doubled with reference to the omnidirectional mode.

- On the other hand, this network was not as efficient as the first network. Heavy traffic caused most queues to keep packets for longer time periods, and this probably accounted for the lower efficiency rates.

The procedure followed in this section differed from previous approaches. In this endeavor, our objective was to keep the number of links unaffected ($|E|$ set of the graph). Although we built the adjacency matrix in exactly the same

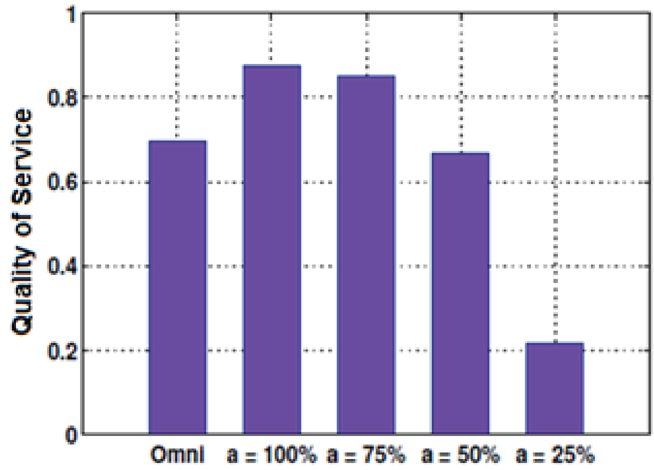

(a) Quality Of Service

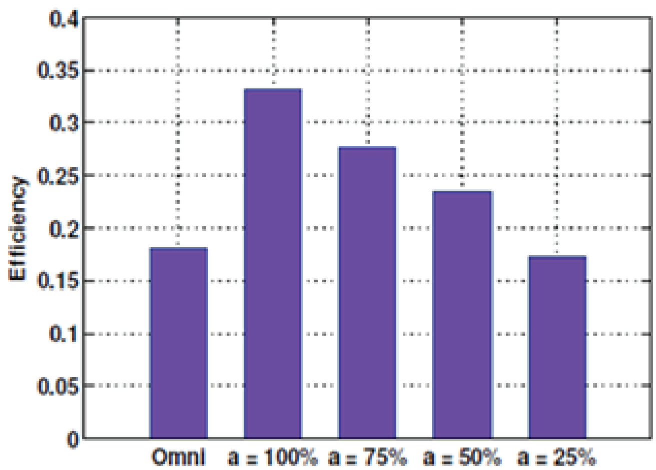

(b) Efficiency

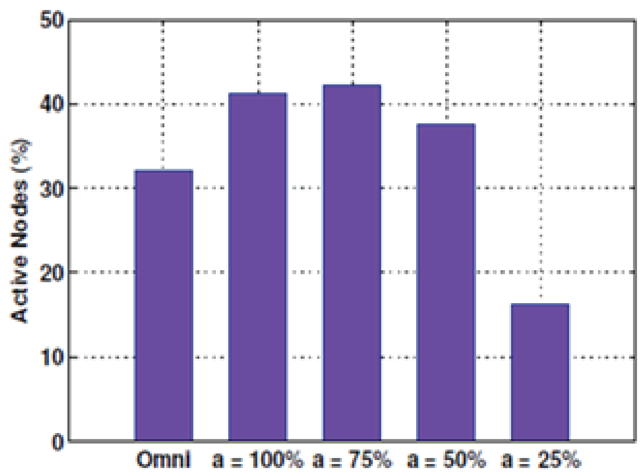

(c) Active Nodes %

Figure 9. The energy consumption: the network performance with respect to transmitted power, node density = $1/100\ \mathrm{m}^2$, $\lambda = 0.5$: (a) quality of service; (b) efficiency; (c) active nodes (%).

way, we modified the transmitted power for each individual node to determine the minimum power required in order for the transmission between each adjacent node pair to be successful. This power value was considerably lower compared to the value used with omnidirectional antennas. For instance, a packet was received under -40 dBm while the threshold set by the receiver equaled -70 dBm: the node transmitting could have saved valuable energy (approximately 10-15 dBm, in this case) by reducing its transmitted power. Modifying the transmitted power was allowed only if all transmissions for this node could be successfully carried out after this modification, which was ensured by setting the transmitted power equal to the minimum power required for every existing link of the node (the complexity of this estimation was $O(NodeDegree)$, as we needed to consider every one-hop neighbor (*NodeDegree*) of the specific node, and find the maximum power required to establish the link).

We then compared the necessary transmitted power when antennas transmitted omnidirectionally compared to the power required when nodes were equipped with smart antennas, enabling them to transmit towards different directions contingent on the target, for various node-density values. We assumed that the network was a sparse sensor network, deploying $N = 50$ nodes, placed at a distance of approximately 10 m from their neighbors. More specifically, we intended to estimate the average transmitted power that ensured connectedness for the network we examined. In this way, we could easily determine a suitable threshold value for the receiver's sensitivity. Therefore, assuming that $R = 10$ m, and after substituting the values for losses, gains, λ, etc., Equation (1) yielded

$$P_{rec}\big|_{dBm} = 10\log\left[\frac{P_t \times 10^{0.3} \times 10^{0.3}}{10^{0.3}}\left(\frac{0.125}{4\pi \times 10}\right)^2\right]; -57 + P_t\big|_{dBm}. \tag{8}$$

The transmitted power was 1 mW, i.e., 0 dBm, and the threshold was set accordingly, i.e., -57 dBm. Figure 9 is a characteristic example of a single network where each node had a different transmitted power, determined as explained above. This distribution was displayed by almost every network of identical node density. Every node required greater transmitted power in the traditional operating mode, which surpassed 40% of the power needed by smart antennas. This difference was close to 2 dB, i.e., the gain difference between the modes.

Finally, two more diagrams are introduced. The first diagram (Figure 10a) demonstrated the necessary transmitted power so that the signals were received with the minimum power required. The second diagram (Figure 10b) illustrated the comparison of the mean transmitted power with regard to node density. Omnidirectional antennas exhibited an average value close to the transmitted power (0 dBm), while smart antennas required less power to establish the same links in the network, with the percentage improvement ranging from 15% to 30%.

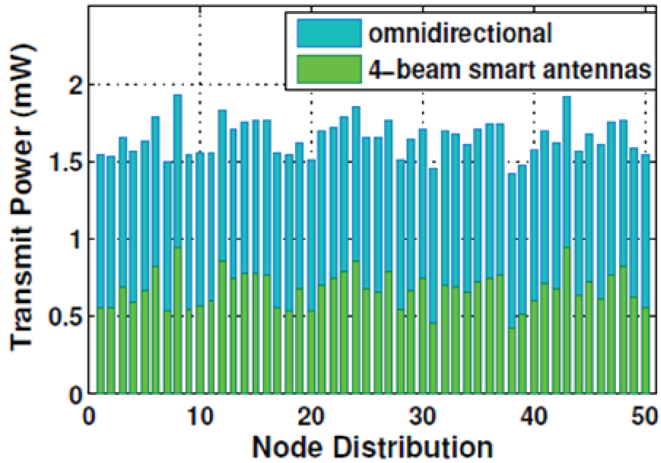

Figure 10a. The transmitted power as a function of the node distribution, node density: $1/100\ \mathrm{m}^2$, $\lambda = 0.5$.

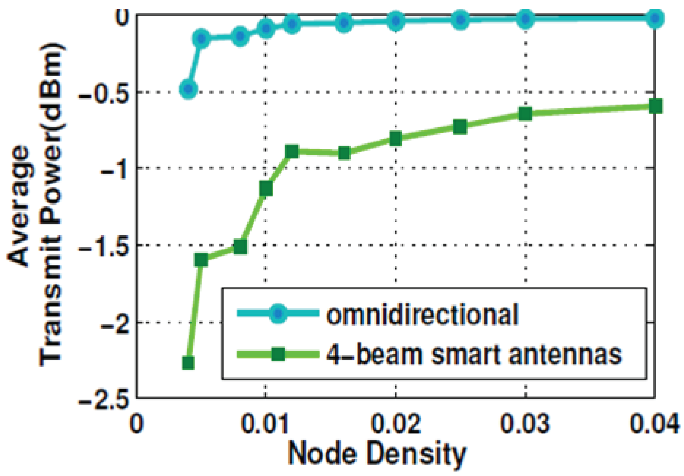

Figure 10b. The transmitted power as a function of the node density, $\lambda = 0.5$.

5. Further Considerations

This section deals with further improvements and extensions of the previously discussed network model, with a view toward assessing the contribution of two alternative approaches. Increasing the number of beams of the smart antennas constitutes the first approach, although a costly approach. The second approach (the hybrid model), which lies in the idea of exclusively installing smart antennas in a small number of the nodes, aims to bridge the gap between cost efficiency and performance enhancement.

5.1 Multi-Beam Smart Antennas

In this section, we discuss the benefits emerging from increasing the number of beams of the smart antennas used in wireless sensor networks. It is understood that an increase in the number of beams will accordingly increase the directionality of the links, yielding lower interference between the nodes-transmitters and, in turn, a smaller number of "blocked" nodes, i.e., nodes within the collision areas of active transmissions. In other words, when node n_1 attempts transmission towards node n_2, every node within the area defined by the radiation pattern of each pair of nodes is rendered unable to transmit data, since the node senses the medium and detects the ongoing information exchange. The state of the node is altered only for as long as the current time slot lasts, as the node is now considered incapable of initiating transmission. However, the node is able to receive data from neighboring nodes.

Computing the total area covered by active transmissions showed that as the number of beams was increased, the network's performance was enhanced, although not proportionally. The evaluation of smart antennas comprising more switching beams was performed using similar metrics as in the four-beam case. The numerical results are illustrated in Figure 11 as functions of the node density for omnidirectional, four-beam, and six-beam smart-antenna-equipped nodes. It was deduced that there was a significant improvement regarding network efficiency, as well as slight improvements regarding quality of service and percentage of active nodes.

5.2 Hybrid Model

In this section, we consider a heterogeneous network, i.e., a network consisting of nodes with different characteristics, some with fewer capabilities and lower cost, and others with better features and higher cost, respectively. This means that we built an adjacency matrix with a slightly different method, so as to include both nodes with omnidirectional antennas and nodes with smart antennas. To attain this, each node was selected with probability p, and was supplied with smart antennas: consequently, the capabilities of the node were modified. Finally, a heterogeneous network that lay between the two types of networks studied in Section 2 was produced.

The purpose of the hybrid approach was to trade-off the deployment of wireless sensor networks and the operating cost against performance. This was because there were a few expensive nodes with higher power resources, while the majority of the rest of the nodes were common nodes, operating in the simplest mode, and thus consuming less power. Herein, we present the figures for three network structures: the "plain" structure, which pointed to homogeneity, and two "hybrid" models, built from nodes with different features (here, probability p denoted the percentage of the nodes that operated with four-beam smart antennas). For instance, $p = 0.20$ meant that approximately 20% of the nodes were equipped with smart antennas. The same explanation stood for $p = 0.50$.

We evaluated the quality of service, efficiency, and the percentage of active nodes, for various p values. As shown in

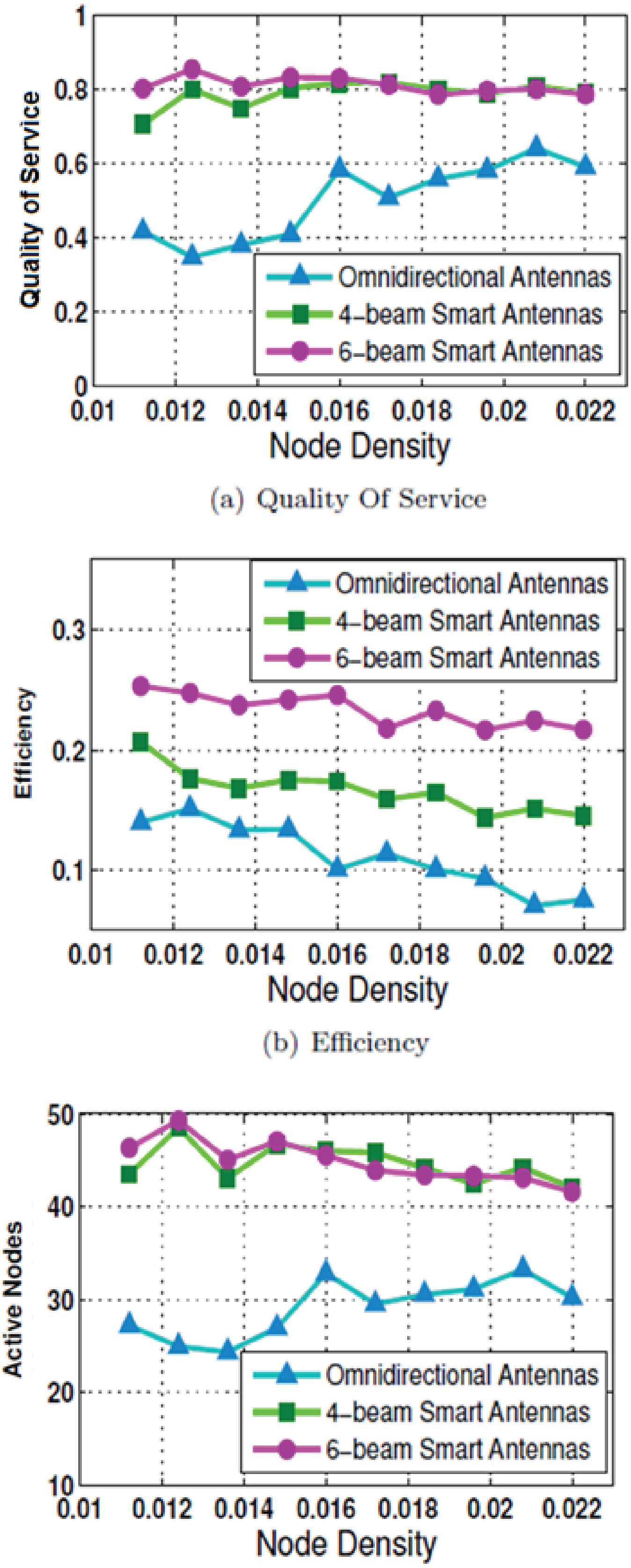

(c) Active Nodes

Figure 11. The network performance as a function of node density for smart antennas, $\lambda = 0.5$: (a) quality of service; (b) efficiency; (c) active nodes.

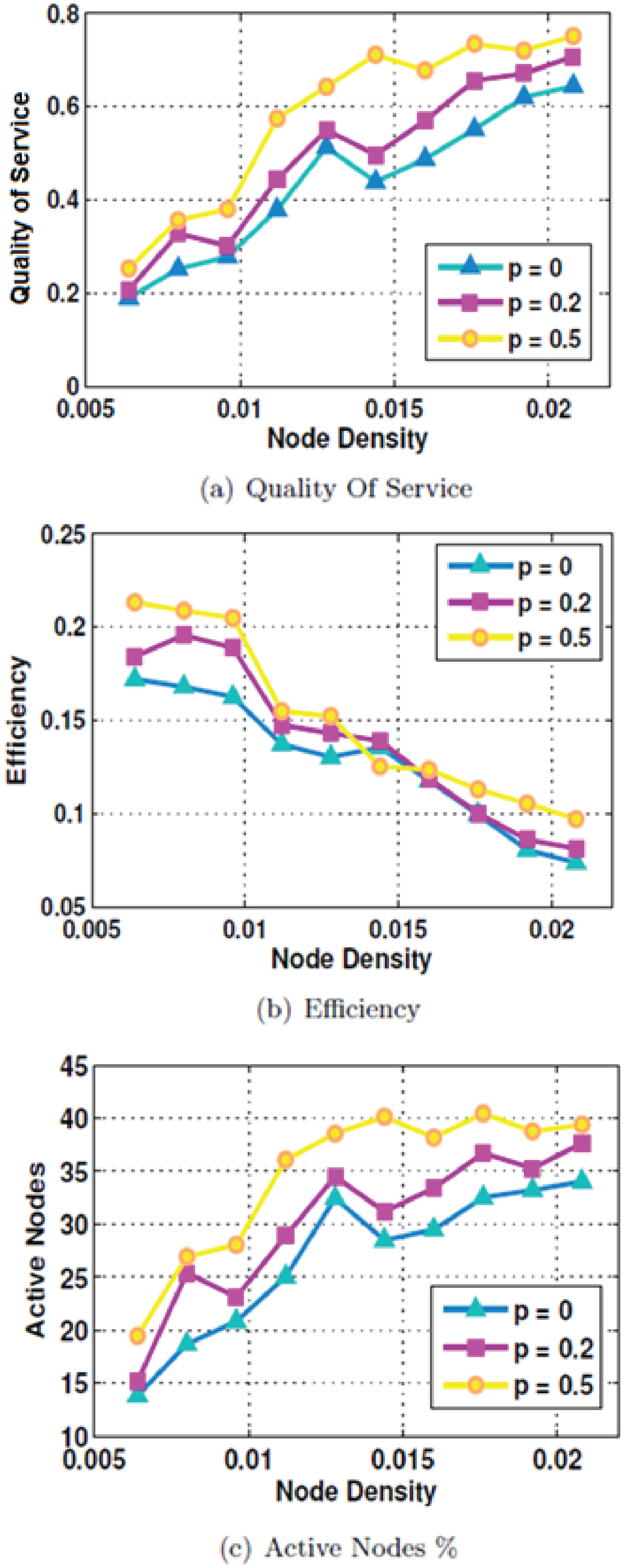

Figure 12. The heterogeneous network performance for the hybrid model as a function of node density, where p is the percentage of smart-antenna-equipped nodes, $\lambda = 0.5$: (a) quality of service; (b) efficiency; (c) active nodes.

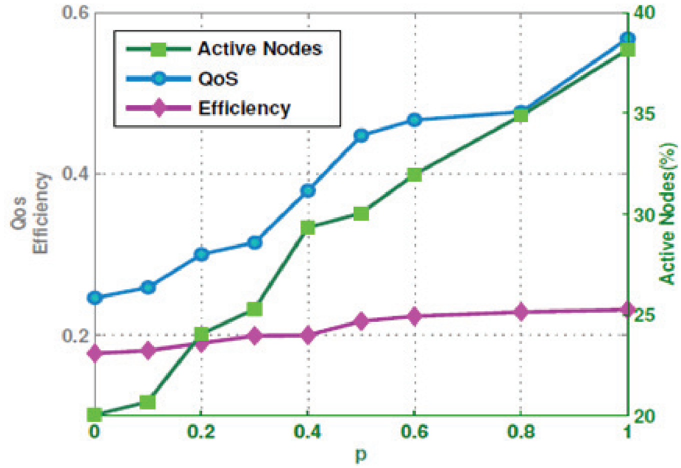

Figure 13. The heterogeneous network performance for the hybrid model as a function of p (the percentage of nodes equipped with smart antennas), node density: $1/100\ \mathrm{m}^2$, $\lambda = 0.5$.

Figure 12, the network performance was enhanced. Nevertheless, this improvement was not as significant as the previously studied network type. The model lay somewhere between the omnidirectional and the smart-antennas mode for the parameter tested, i.e., node density. The quality of service, the efficiency, and the percentage of active nodes all increased, however without reaching the values of the smart-antennas mode studied in Section 3.1. Let us assume, for instance, that the node density was 0.01. In this case, the classic approach provided a value of 80% for the quality of service, 20% for the efficiency, and 40% for the active nodes percentage metrics. The corresponding values for the hybrid model were 70%, 15%, and 30%, respectively. Finally, it should be noted that in Figure 10b, at point six for $p = 0.50$, the efficiency seemed lower compared to other p values. Again, this was due to a slight averaging fluctuation, and did not affect the discussed trends and conclusions.

The comparison between different hybrid models revealed a small difference between hybrid networks, although the improvement was noticeable compared to the plain network. From Figure 13, it followed that the improvement in quality of service, efficiency and active nodes percentage was considerable, even for a small number of smart antennas used. This indicated that the proposed approach is valuable, even in a hybrid (and more cost-efficient) approach.

These results, together with a cost analysis of deploying smart antennas over wireless sensor networks, could be used in order to estimate the optimal tradeoff point between cost and performance, and to determine the number of smart antennas that should be used in the network.

6. Conclusion

In this paper, it was proposed that the performance of wireless sensor networks can be improved in terms of various metrics in the case where smart antennas are used in the network nodes. A simulator was also built, in order to numerically evaluate the proposed approach. Numerical results were presented confirming our expectations. They indicated that the performance of a wireless sensor network is significantly improved with respect to quality of service, efficiency, active nodes percentage, and energy consumption. Wireless sensor networks equipped with smart antennas demonstrated improved features even in the case where these antennas were only installed in a fraction of the nodes (the hybrid network model). It was impressive that the performance of smart-antenna-equipped wireless sensor networks was doubled with respect to an omnidirectional-only network, while increasing the number of beams resulted in even higher performance. Furthermore, it was found that in general, the performance of the network was independent of the network size, which guaranteed scalability. The proposed approach revealed the importance of incorporating smart antennas into wireless network systems, yielding desirable results without modifying the features that characterize a network as a wireless sensor network (self-organization, limited transmission range, highly clustered nodes). It has been shown that smart antennas can be designed to fit a broader range of applications, catering to higher efficiency and improved quality, at almost no cost. It is considered that this alternative could open new avenues in research, offering incentives for innovative ideas as well as further improvements, and alterations in existing projects.

7. Acknowledgements

This research has been supported in part by the European-Commission-funded projects HMFM – "Hear Me Feel Me – Compensating for Eyesight with Mobile Technology," Project No. AAL-2008-1-041, and DITSEF "Digital & Innovative Technologies for Security & Efficiency of First Responder Operations," Contract No. 225404- Programme: Joint Call FP7-ICT-SEC 2007-1.0, and in part by an NCSR Demokritos' Post-Graduate Fellowship.

8. References

1. C. N. Raghavendra, K. M. Sivalingham, and T. Znati, *Wireless Sensor Networks*, New York, Springer Science and Business Media Inc., 2004.

2. I. F. Akyildiz, W. Su, Y. Sankarasubramaniam, and E. Cayirci, "Wireless Sensor Networks: A Survey," *Computer Networks Journal*, **18**, 2, 2002, pp. 393-422.

3. S. Misra, S. C. Misra, and I. Wounqanq, *Guide to Wireless Mesh Networks*, Berlin, Springer, December 2010.

4. F. L. Lewis, "Wireless Sensor Networks," in Diane Cook and Sajal Das (eds.), *Smart Environments: Technologies, Protocols and Applications*, New York, John Wiley and Sons, 2004.

5. E. H. Callaway, *Wireless Sensor Networks: Architectures and Protocols*, Boca Raton, FL, CRC Press, 2004.

6. S. A. Mitilineos, D. M. Kyriazanos, O. E. Segou, J. N. Goufas, and S. C. A. Thomopoulos, "Indoor Localization with Wireless Sensor Networks," *Progress in Electromagnetic Research*, **109**, 2010, pp. 441-474.

7. R. Iyer and L. Kleinrock, "QoS Control for Sensor Networks," IEEE International Conference on Communications, **1**, 2003, pp. 517-521.

8. Q. Zhang and Y. Q. Zhang, "Cross-Layer Design for QoS Support in Multihop Wireless Networks," *Proceedings of the IEEE*, **96**, 1, 2008, pp. 64-76.

9. J. Frolik, "QoS Control for Random Access Wireless Sensor Networks," Proceedings of the Wireless Communications and Networking Conference, **3**, March 21-25, 2004, pp. 1522-1527.

10. Q. Zhao and L. Tong, "QoS-Specific Information Retrieval for Densely Deployed Sensor Network," Proceedings of 2003 Military Communications International Symposium, Boston, MA, October 2003, pp. 1-5.

11. I. Rhee, A. Warrier, M. Aia, and J. Minz, "Z-MAC: A Hybrid MAC for Wireless Sensor Networks," Technical Report, Department of Computer Science, North Carolina State University, April 2005.

12. A. Kouba, M. Alves, and E. Tovar, "i-GAME: An Implicit GTS Allocation Mechanism in IEEE 802.15.4," Proceedings of the 18th European Conference on Real-Time Systems, July 2006, pp. 183-192.

13. E. Felemban, C. Lee, and E. Ekici, "MMSPEED: Multipath Multi-SPEED Protocol for QoS Guarantee of Reliability and Timeliness in Wireless Sensor Networks," *IEEE Transactions on Mobile Computing*, **5**, 6, June 2006, pp. 738-754.

14. V. Srivastava, and M. Motani, "Cross-Layer Design: A Survey and the Road Ahead," *IEEE Communications Magazine*, **43**, 12, 2005, pp. 112-119.

15. R. Wattenhofer, L. Li, Bahl, and P. Wang, "Distributed Topology Control for Power Efficient Operation in Multi-Hop Wireless Ad-Hoc Networks," Proceedings of the 20th Annual Joint Conf. of the IEEE Computer and Communications Societies, INFOCOM, **3,** April 22-26, 2001, pp. 1388-1397.

16. P. Santi, *Topology Control in Wireless Ad Hoc and Sensor Networks*, Chichester, Wiley, 2005.

17. M. Burkhart, P. von Rickenbach, R. Wattenhofer, and A. Zollinger, "Does Topology Control Reduce Interference?,"

Proceedings of 5th ACM International Symposium on Mobile Ad Hoc Networking and Computing, MOBIHOC 2004, 2004, pp. 9-19.

18. P. von Rickenbach, S. Schmid, R. Wattenhofer, and A. Zollinger, "A Robust Interference Model for Wireless Ad Hoc Networks," 5th International Workshop on Algorithms for Wireless, Mobile, Ad Hoc and Sensor Networks (WMAN), Denver, CO, April 2005, p. 239.

19. A. K. Sharma, N. Thakral, S. K. Udgata and A. K. Pujari, "Heuristics for Minimizing Interference in Sensor Networks," Proceedings of ICDCN 2009, 2009, pp. 49-54.

20. H. Jang, "Applications of Geometric Algorithms to Reduce Interference in Wireless Mesh Networks," *International Journal on Applications of Graph Theory in Wireless Ad Hoc Networks and Sensor Networks (Graph Hoc)*, **2**, 1, March 2010, pp. 62-85.

21. J. Tang, G. Xue, and W. Zhang, "Interference-Aware Topology Control and QoS Routing in Multi-Channel Wireless Mesh Networks," Proceedings of the 6th ACM International Symposium on Mobile Ad Hoc Networking and Computing, 2005, pp. 68-77.

22. J. C. Liberti and T. S. Rappaport, *Smart Antennas for Wireless Communications: IS-95 and Third Generation CDMA Application*, Upper Saddle River, NJ, Prentice Hall, 1999.

23. A. Lozano, F. R. Farrokhi, and R. A. Valenzuela, "Lifting the Limits on High-Speed Wireless Data Access Using Antenna Arrays," *IEEE Communications Magazine*, **39**, 9, September 2001, pp. 156-162.

24. J. H. Winters, "Smart Antennas for Wireless Systems," *IEEE Personal Communications*, **1**, February 1998, pp. 23-27.

25. B. Sklar, "Rayleigh Fading Channels in Mobile Digital Communication Systems Part I: Characterization," *IEEE Communications Magazine*, **35**, 7, July 1997, pp. 90-100.

26. A. Paulraj, R. Nabar, and D. Gore, D., *Introduction to Space-Time Wireless Communications*, Cambridge, Cambridge University Press, 2003.

27. G. L. Stuber, J. R. Barry, S. W. McLaughlin, Y. G. Li, M. A. Ingram, and T. G. Pratt, "Broadband MIMO-OFDM Wireless Communications," *Proceedings of the IEEE*, **92**, 2, February 2004, pp. 271-294.

28. S. Bellofiore, C. A. Balanis, J. Foutz, and A. S. Spanias, "Smart-Antenna Systems for Mobile Communication Networks Part 1: Overview and Antenna Design," *IEEE Antennas and Propagation Magazine*, **44**, 3, June 2002, pp. 145-154.

29. S. A. Mitilineos and C. N. Capsalis, "A New, Low-Cost, Switched Beam and Fully Adaptive Antenna Array for 2.4 GHz ISM Applications," *IEEE Transactions on Antennas and Propagation*, **AP-55**, 9, September 2007, pp. 2502-2508.

30. S. A. Mitilineos, K. S. Mougiakos, and S. C. A. Thomopoulos, "Design and Optimization of ESPAR Antennas via Impedance Measurements and a Genetic Algorithm," *IEEE Antennas and Propagation Magazine*, **51**, 2, April 2009, pp. 118-123.

31. S. A. Mitilineos, S. C. A. Thomopoulos, and C. N. Capsalis, "On Array Failure Mitigation with Respect to Probability of Failure, Using Constant Excitation Coefficients and a Genetic Algorithm," *IEEE Antennas and Wireless Propagation Letters*, **5**, 2006, pp. 187-190.

32. R. Albert and A-L. Barabasi, "Statistical Mechanics of Complex Networks," *Department of Physics*, **74**, 47, January 2002, pp. 47-97.

33. W. An, F. Shao, and H. Meng, "The Coverage-Control Optimization in Sensor Network Subject to Sensing Area," *Journal of Computers and Mathematics with Applications*, **57**, 4, February 2009, pp 529-539.

34. T. H. Cormen, C. E. Leiserson, R. L. Rivest, and C. Stein, "Dijkstra's algorithm," in T. H. Cormen, C. E. Leiserson, R. L. Rivest, and C. Stein (eds.), *Introduction to Algorithms*, New York, McGraw-Hill, 2001, pp. 595-601.

Introducing the Feature Article Authors

Evangelia Skiani was born in Athens, Greece, in 1986. She received her Diploma in Electrical and Computer Engineering (ECE) from the National Technical University of Athens (NTUA), Greece, in November 2009, and her MSc in Electrical Engineering from Columbia University, New York, USA, in May, 2011. She worked as an internship fellow with the National Center for Scientific Research "Demokritos," Greece (IIT-NCSR) from March 2010 to August 2010. She is currently a PhD candidate at Columbia University, School of Graduate Arts and Sciences, USA. Her main research interests lie in the areas of networking and communications, network modeling and analysis, and large-scale computing systems.

Stelios A. Mitilineos was born in Athens, Greece, in 1977. He received the Diploma in ECE from NTUA in October 2001, and his PhD from NTUA in June 2007, with a fellowship from the Institute of Informatics and Telecommunications, National Center for Scientific Research "Demokritos," Greece (IIT-NCSR). He was a fellow post-doc researcher with IIT-NCSR from 2008 to 2011. He is currently an appointed tenure-track lecturer with the Technological Education Institute of Piraeus, Greece, where he is involved in teaching as well as active research on current European and national projects. His main research interests are in the areas of antennas and propagation, smart antennas, and microwave components, mobile communications and mobile channel simulation, and position location.

Stelios C. A. Thomopoulos received his Diploma of Electrical and Mechanical Engineering in July 1978 from NTUA, Greece. He then earned his MS in January 1981 and his PhD in January 1983, both in Electrical Engineering, from the Department of Electrical and Computer Engineering of the State University of New York at Buffalo. From 1983 to 1992, he was with the faculty of the Electrical Engineering Department of Southern Illinois University, first as an Assistant Professor (1983-89), then as an Associate Professor (1989-1990), and then as an Adjunct Associate Professor (1990-92). In August 1989, he joined the faculty of the Electrical and Computer Engineering Department at the Pennsylvania State University, on leave from Southern Illinois University, and remained with the faculty of Penn State University until 1996. Since July of 1998, he has been with the National Center for Scientific Research (NCSR) "Demokritos," where he currently is Director of Research in the Integrated Systems Laboratory and Associate Director of II&T. Prof. Thomopoulos is credited with over 160 publications in peer-reviewed professional journals and conference proceedings, and over 570 citations by third-party publications in peer-reviewed papers in the period between 1987 and 2006. He holds US Patent No. 5,978,495 for the design and implementation of a fingerprint-recognition system. His current interests include location-based systems, with emphasis on transport on demand and navigation.

Changes of Address or Delivery Problems

Information regarding subscriptions and addresses is managed by IEEE headquarters. It is *not* maintained, nor can it be changed, by any member of the *Magazine* staff. If you are a member of the IEEE, your subscription is sent to the address in your IEEE member record. Your address can be confirmed or updated by visiting the Web page dealing with delivery of IEEE publications:

http://www.ieee.org/about/help/subscriptions.html

This page also has information about publication delivery, and a link to an online form that can be used to inquire about missing or delayed publications:

http://www.ieee.org/about/help/publication_inquiry.html

You can also update your address information by contacting IEEE headquarters: Member Address Records, IEEE Headquarters, 445 Hoes Lane, Piscataway NJ 08855-1331 USA; Tel: +1 (908) 981-0060 or +1 (800) 678-4333; Fax: +1 (908) 981-9667; E-mail: address.change@ieee.org. If you are an institutional or other non-member subscriber, contact IEEE Customer Service at the above address, telephone, and fax numbers; E-mail: customer.service@ieee.org.

Please do *not* send requests related to the above items to any member of the *Magazine* Staff.

Getting the *Magazine* by Air Freight

Air freight delivery of the *IEEE Antennas and Propagation Magazine* is available to subscribers in IEEE Regions 8-10. The cost was recently $44.00 per year. This can be added to a member's subscription (and the current cost verified) via the Web at http://www.ieee.org/web/aboutus/help/member_support.html.